IEEE Transactions on Nuclear Science, Vol. NS-28, No. 3, June 1981

FINAL DESIGN OF THE MAGNETIC FIELD FOR THE K-800 SUPERCONDUCTING CYCLOTRON AT MSU

F.G. Resmini, G. Bellomo, H.G. Blosser, E. Fabrici, D. Johnson

Cyclotron Laboratory, Michigan State University
East Lansing, MI 48824

Introduction

Substantial progress has been made in recent months in the design of the K800 cyclotron at MSU. As a consequence, the geometry is somewhat different from that outlined in (1) with implications on magnetic field properties, beam dynamics and extraction. Injection of beams from the K500 has not been affected by said modifications and we refer to (2) for all details.

It is the purpose of this paper to review the finalized design of the K800 and the rationale for the choices which have been made, together with their implications on the machine performance.

Review of the K800 Characteristics

As well known, the K800 is mainly intended as a booster for the K500 cyclotron, now near completion, although operation with an internal ion source is also anticipated. The energies will be 200 MeV/n for fully stripped light ions and up to 30 MeV/n for heavy ions, depending upon the available charge states from the K500.

The parameters of the machine are listed in Table I. The main differences with respect to ref. 1 are:

- the increase in pole radius from 41" to 42",
- the increase in the hill gap from 2.5" to 3",
- the increase in the hill width, at outer radii, from 46° to 51°.

The rationale for these choices will be discussed later. The operating diagram in the (B_o, Z/A) plane is shown in Fig. 1, all limits are indicated in a straightforward way.

Table I. Main K800 Parameters.

Pole radius	: 42"
Sectors	: 3, 46° wide, up to R=37.15". Flaring to 51° wide between R=37.15" and R=40.2".
Spiral constant	: 1/13 rad/inch (approx)
Minimum hill gap	: 3"
Maximum valley gap	: 36"
Min-max operating average field	: 30-50 kgauss
Yoke height	: 115"
Yoke inner and outer diameters	: 118" - 175"
R.F. frequency range	: 9-32 MHz
Harmonic operating modes	: 1st, 2nd
Peak dee voltage	: 200 kV
No of trim coils	: 22
Max current in any trim coil	: 400A
Max total trim coil power	: 70 kW
K at 50 kgauss	: 1200
$K_{Focusing}$	: 400

Twelve ions were chosen as representative ones on the operating diagram contours, as shown by dots in Fig. 1, in order to investigate the field trimming, equilibrium orbit properties and extraction.

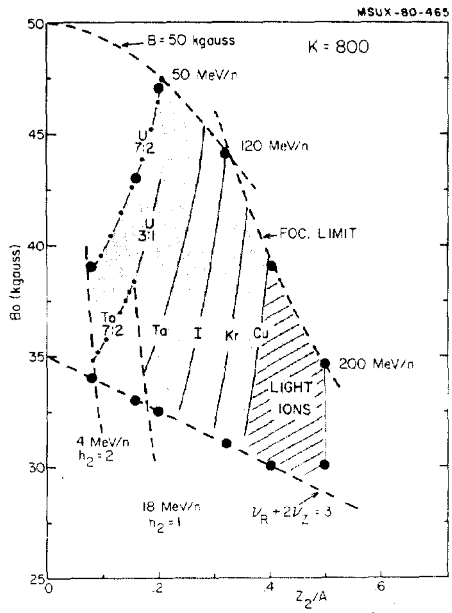

FIG. 1. Operating diagram of the K800 in the (B_o, Z/A) plane. Shown are focusing and bending limits and the low field limit due to the $\nu_R + 2\nu_V = 3$ resonance.

Main Coil Design

The coil parameters are listed in Table II. The main variation with respect to (1) is the increase of the minimum coil distance from the median plane, from 1.5" to 2". This increase allows more axial space for the

Table II. Main Coil Parameters

Inner coil radius	: 45.5"
Outer coil radius	: 51.5"
Coil total height	: 26.5"
Coil splitting	: Two sections, indep. excited
Height of section α (closer to med. plane)	: 16" (60% of total)
Height of section β (away from med. plane)	: 10.5" (40% of the total)
Minimum coil distance from med. plane	: 2"
Bobbin thickness	: .95"
Banding thickness	: 2", Aluminum alloy
Vacuum tank inner radius	: 42.25", 1" thick
Vacuum tank outer radius	: 58.5"
Cryostat total height	: 69"
Maximum current density in the coils	: 3500 A/cm^2
Amper turns at 3500 A/cm^2	: 7.2 10^6
Conductor	: NbTi, monolithic type
Conductor cross section	: .207" x .15"
Nominal Max current in conductor	: 1000 A
Overall copper to super-conductor ratio	: 25:1

insertion of the extraction elements, especially the magnetic channels, and has thus been selected. Independent excitation of the two coil sections allows proper fitting of the isochronous field for all different ions and center field values. The resulting operating diagram of the machine in terms of the current densities J_α and J_β is presented in Fig. 2. As apparent from the figure, J_β must go to a negative value with respect to J_α for many of the most relativistic ions, i.e. for Z/A from 0.3 to .5 and for the energies close to the focusing limit.

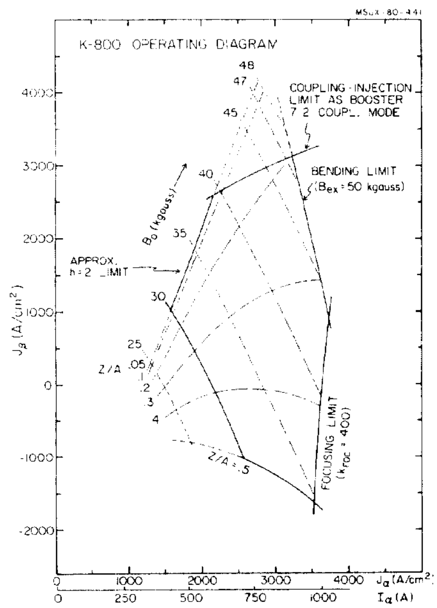

FIG. 2. Operating diagram of the K800 cyclotron in terms of the current densities in the two main coil sections. (α denotes the section close to the median plane, β the one farther away.) Constant B_0 and Z/A lines are also shown.

The conductor choice has been dictated mainly by the need to keep the coil inductances within reasonable limits. We have selected for the current maximum nominal value of ≈1000 A, i.e. somewhat higher than the one (700 A) for the K500. Accordingly, the conductor, of the type, shall have dimensions of .207" x .15", with an overall copper to superconductor ratio of 25:1. The monolithic superconductor will be inserted in a U-shaped slot in the copper of dimensions .044" x .066".

With this choice of conductor the inductances at the max field level, i.e. $J_\alpha = J_\beta = 3500$ A/cm will be: $L_\alpha = 51$ H, $L_\beta = 18.8$ H, $M_{\alpha\beta} = 19$ H, for a total stored energy of ≈61 MJ.

The coil winding technique shall be essentially similar to the one used for the K500. Details on anticipated forces and stresses are given in ref. 3.

Pole tip Design

The median plane geometry of the sectors is shown in Fig. 3, and their radial profiles for both hills and valleys, in Fig. 4.

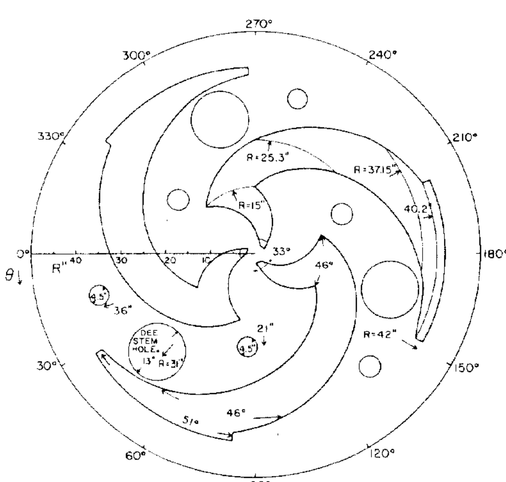

FIG. 3. Median plane geometry of the K800 sectors. Hills are split into five sections, whose radii are indicated. Also shown are the dee stem hole and the trimming and coupling capacitor holes in the valleys.

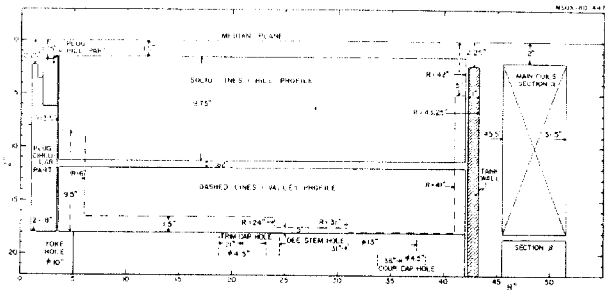

FIG. 4. Hill and valley profiles as a function of radius. Also shown are details of the tank wall and the main coil position.

The increase in pole radius, to 42", was prompted by the fact that if the .25" radial clearance between the vacuum tank and the pole is set at 41" as originally devised, the local reduction in the average field and flutter is too high and cannot be properly compensated. The tank wall thickness was thus reduced to 1", down from the anticipated 2", and consequently the .25" radial gap is between 42" and 42.25" where its effects on the field are more tolerable.

The increase of the minimum hill gap to 3" was dictated by extraction considerations. As discussed later, it is necessary to move the deflectors to smaller radii as the field level is lowered. We have thus increased the hill gap to 3", and at the same time reduced the axial space occupied by the last trim coil by .5". This is accomplished by having just one layer of 1/4" square conductor for this particular trim coil, instead of the two layers used elsewhere (and in the K500 as well). The deflector can then slide inward over the last trim coil and still have a sufficient axial clearance.

The valleys, whose nominal gap is 36", are shimmed in order to reach the desired slope of the average field, all details being given in Fig. 4. The center hole, in the sector region, has a 7" diameter as in the K500, but in the pole, i.e. starting at a distance of 18" from the median plane, it increases to 10" diameter. This larger hole is desirable for a possible axial injection system. The plug design follows closely that of the K500, being composed of a cylindrical part and a hill part.

Holes are provided for R.F. purposes, as shown in Fig. 3. In addition there are twenty two holes along each side of each hill, i.e. 44 holes/sector, of .75" diameter, for the leads of the 22 trim coils anticipated in the machine. These holes are not shown in the figures.

Details of the hill width can be seen in Fig. 3 and in Table I. Note that the sector is radial for the last 1.8", a feature already anticipated in (1), in order to shift outward, as much as possible, the $\nu_R + 2\nu_z = 3$ resonance. As shown also in Fig. 3, the transition between the two spirals, at R = 15", has been made sharp instead of the smooth one envisaged in (1). This way both the sectors and the trim coils, which will be wound around the latter, are easier to fabricate.

For the purpose of easy machining the hill profile has been fitted with arcs of circles. It was found necessary to split the sectors in 5 parts, as indicated in Fig. 3, where the values of the separation radii are also noted. More details on the pole tip geometry can be found in ref. 3.

Field Trimming and Equilibrium Orbit Properties

Fitting of the isochronous field for the different ions was carried out on the basis of the magnetic fields calculated according to the geometry discussed above. Details on the procedure are given in Ref. 3.

A summary of the results for the twelve ions chosen along the boundary of the operating diagram is given in

Fig. 5. Both current densities J_α and J_β, the trim coil power and the relevant energy/nucleon are given for each ion. Currents are always below a maximum operating limit of 400 A for any trim coil.

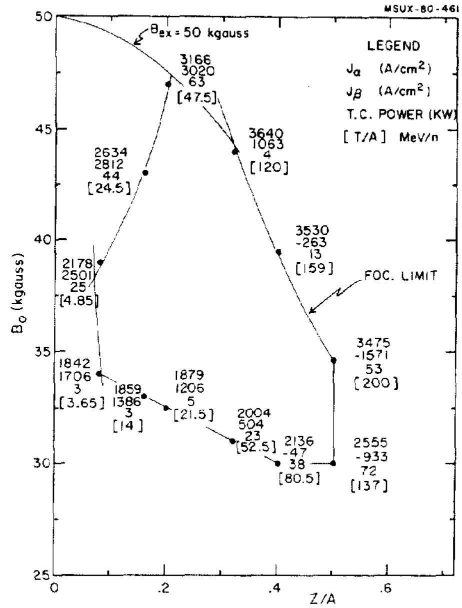

FIG. 5. Required main coil currents, and trim coil power for the twelve representative ions on the (B_o, Z/A) operating diagram.

An example of the resulting total average fields, axial focusing frequencies and accelerating phase is shown in Fig. 6 for fully stripped light ions, Z/A = .5, and two different center field levels. The two levels of 34.6 and 30 kgauss correspond to the maximum and minimum values for these ions and to a final energy of 200 and 137 MeV/n respectively. As shown by the phase curves, the fields thus obtained have excellent isochronous properties. In correspondence of the transition region between the two spirals at R = 15", and also just before the extraction, we accelerate above isochronism in order to enhance the axial focusing there. The maximum negative phase shift thus introduced, is about 25°, the corresponding minimum ν_Z value being about .2. For the most relativistic ions, extraction occurs typically at a positive phase not exceeding ≈30°.

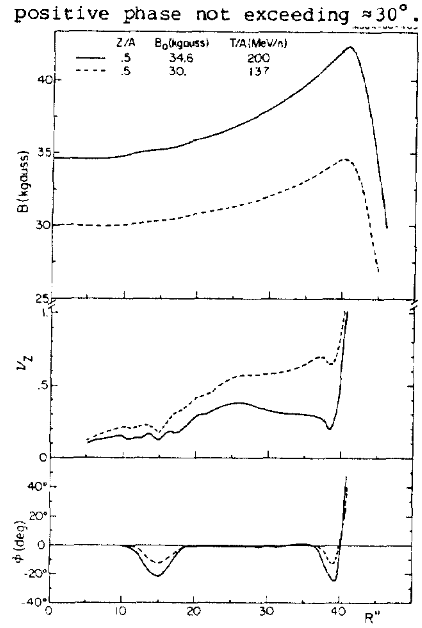

FIG. 6. Average total field, focusing frequency, and accelerating phase for fully stripped light ions at two different center field levels.

Extraction must take place before the crossing of the $\nu_R + 2\nu_Z = 3$ resonance, which shifts inwards at low fields. How this happens is shown in Fig. 7 for Z/A = .5 and Z/A = .32 ions, where the $\nu_R + 2\nu_Z$ values are plotted as a function of the equilibrium orbit radius. For every ion both the minimum and maximum operating fields are considered. As anticipated before, extraction must take place at progressively inner radii, the lower the field. As noted from Fig. 7, the radial movement involved is of the order of .6"/.7". It is this requirement that prompted us to increase the hill gap to 3" and reduce the last trim coil to one layer only.

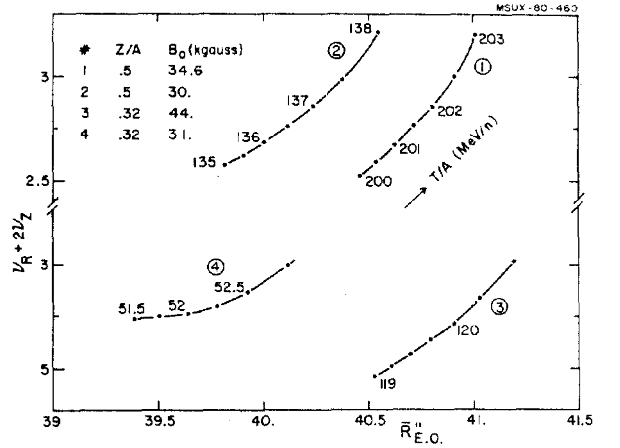

FIG. 7. $\nu_R + 2\nu_Z$ values near extraction for Z/A = .5 and Z/A = .32 ions, as a function of radius. Cases with both minimum and maximum center field values are presented for each ion.

Extraction

The extraction scheme now envisaged involves two electrostatic deflectors instead of three. Nine magnetic channels of the passive type used in the K500 are provided along the extraction path.

A list of the azimuthal position of each element, the maximum electric field in the deflectors, and the values of the bias field and magnetic field gradients in the channels is given in Table 3. Their position can be easily recognized by looking at Fig. 3.

Table III. Extraction Element Parameters

Element	θ_{in} (deg)	θ_{fin} (deg)	E_{MAX} (kv/cm)	B (kgauss)	$\partial B/\partial x$ (kgauss/inch)
E_1	32	92	140	–	–
M_1	150	160	–	-2	5.8
E_2	162	198	140	–	–
M_2	200	212	–	-2	5.8
M_3	260	266	–	-2	7.5
M_4	270	276	–	-2	7.5
M_5	293	299	–	-2	7.5
M_6	310	316	–	-2	5.8
M_7	318	324	–	-2	5.8
M_8	326	332	–	-2	9
M_9	340	346	–	-2	9

The performance of this system looks very satisfactory. Beams are radially and axially confined to ±.10" along the entire extraction trajectory, which encompasses about 330°.

References

1. Conceptual Design Report for Phase II of a National Superconducting Cyclotron Laboratory for Research with Heavy Ions, Internal Report MSUCL-282 and references herein.
2. G. Bellomo, E. Fabrici and F.G. Resmini. Injection Studies for the K800 Superconducting Cyclotron at MSU, IEEE Trans. on Nucl. Sci. NS-26 (1979), 2090.
3. Final Design of the K800 Magnetic Field, G. Bellomo, H.G. Blosser, E. Fabrici, D. Johnson, F.G. Resmini, MSUCP-35, January 1981.